Support information

Facile electrodeposition of cauliflower-like S-doped nickel microsphere films as highly active catalysts for electrochemical hydrogen evolution

J.R. Zeng[a], M.Y. Gao[a], Q.B. Zhang[a,b*], C. Yang[a], X.T. Li[a], W.Q. Yang[a], Y.X. Hua[a,b], C.Y. Xu[a,b], Y. Li[a,b]

[a] Key Laboratory of Ionic Liquids Metallurgy, Faculty of Metallurgical and Energy Engineering, Kunming University of Science and Technology. Kunming, 650093, P.R. China

[b] State Key Laboratory of Complex Nonferrous Metal Resources Cleaning Utilization in Yunnan Province, Kunming 650093, P.R. China

*Corresponding author. Tel: +86-871-65162008; fax: +86-871-65161278.

E-mail address: qibozhang@kmust.edu.cn (Q.B. Zhang)

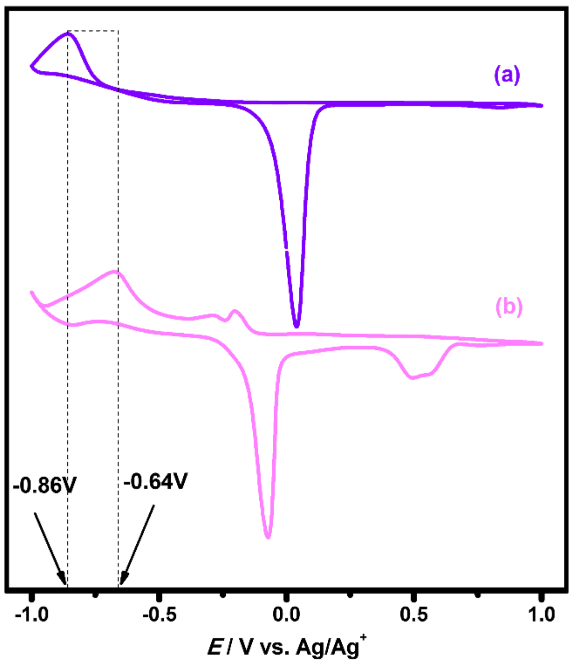

Figure S1. CVs of ethaline with 0.01 M $NiCl_2 \cdot 6H_2O$ in the absence (a) and presence of 0.02 M thiourea (b), recorded on a Pt electrode at 333 K under a scan rate of 0.02 V s^{-1}.

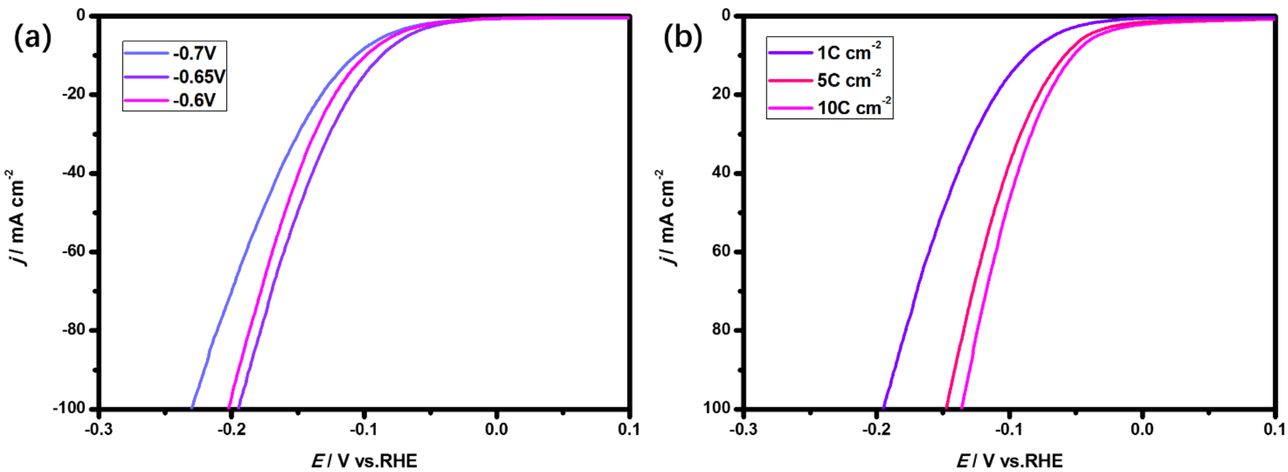

Figure S2. LSV curves of NiS_x/CW deposited in diferent potential with a charge density of 1 C cm^{-2}. The LSV of NiSx/CW deposited in different electric charge density at the applied potential of -0.65 V vs. Ag/Ag^+.

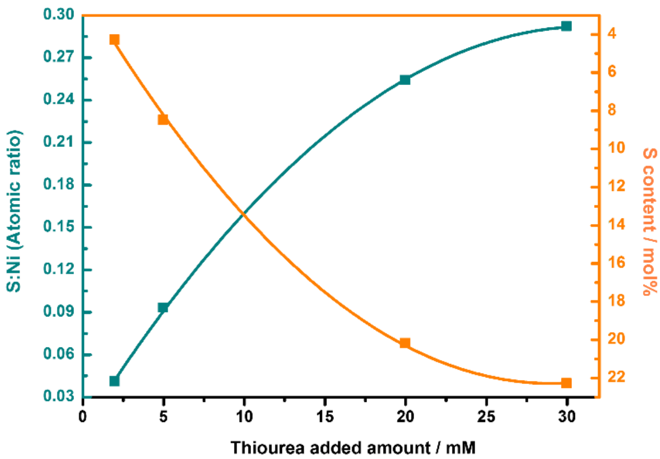

Figure S3. ICP-MS survey of the as-deposited NiS_x/CW with different amounts of S doping obtained at -0.65 V vs. Ag/Ag^+ with a charge density of 10 C cm^{-2} at 333 K.

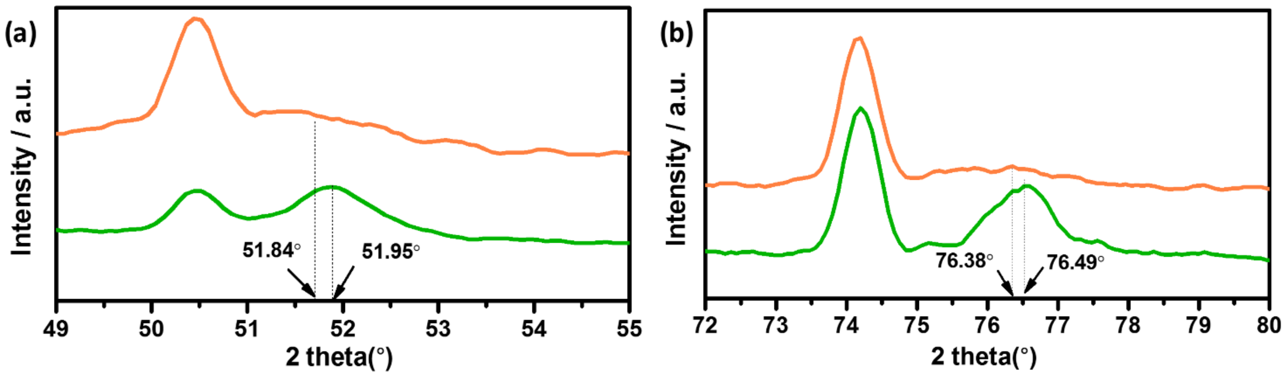

Figure S4. XRD patterns of deposited pure Ni/CW and $NiS_{0.25}$/CW.

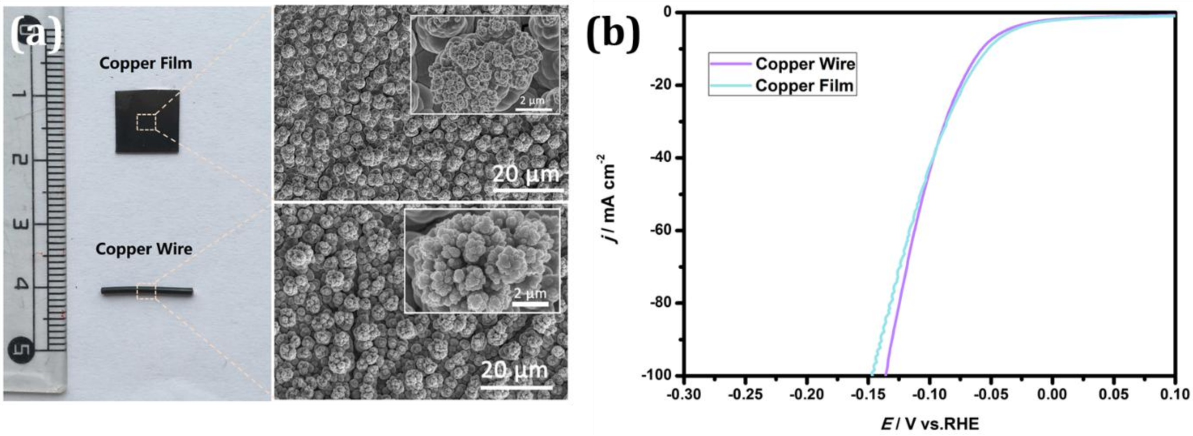

Figure S5. (a) Photographs and SEM images of $NiS_{0.25}$/CW (prepared at -0.65 V vs. Ag/Ag^+ with a charge density of 10 C cm^{-2} at 333 K in 100 mM $NiCl_2 \cdot 6H_2O$ + 20 mM thiourea/Ethaline) grown on copper wire and copper foil. (b) The corresponding LSV curves performed in 1.0 M KOH at 298 K with a scan rate of 2 mV s^{-1}. Theses resluts revealed that the shape of substrate (wire or foil) had little influence on the resultant deposit morphology and associated HER catalytic performance.

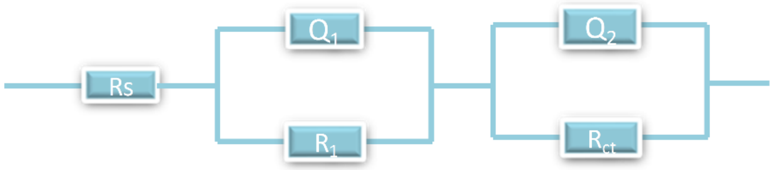

Figure S6. Equivalent circuit used for the HER. R_1 and Q_1 are corresponded with electrode porosity, R_{ct} and Q_2 are corresponded with kinetics of the HER process.

Table S1. Fitted parameters of equivalent circuit as given in Figure S5 for fitting the EIS data (Figure 4c).

Electrode	R_s (Ω cm^2)	R_1 (Ω cm^2)	R_{ct} (Ω cm^2)
Pure Ni	0.637	0.141	202.4
$NiS_{0.04}$	0.854	0.946	0.130
$NiS_{0.09}$	0.957	0.736	0.129
$NiS_{0.25}$	0.819	0.640	0.088
$NiS_{0.29}$	0.899	0.685	0.118

Table S2. Arverage thickness, mass loading and associated mass acitivity of various catalysts.

Electrode	Arverage thickness /μm	Mass loading /mg cm^{-2}	Mass activity at η = -200 mV /A·g^{-1}
Pure Ni	4.04	2.9	0.86
$NiS_{0.04}$	15.3	3.1	50.4
$NiS_{0.09}$	17.2	3.4	42.6
$NiS_{0.25}$	21.8	3.6	66.8
$NiS_{0.29}$	23.2	4.2	46.5

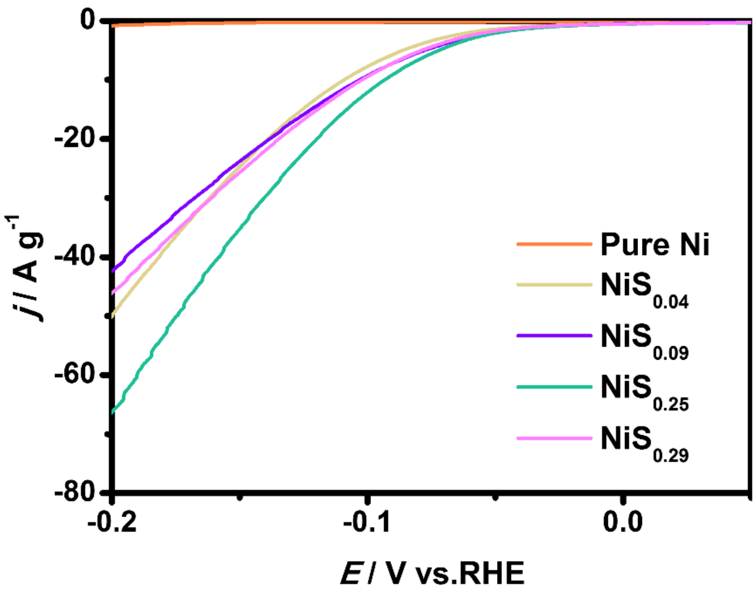

Figure S7. LSV curves of NiSx/CW with different amounts of S doping normalized by mass loading.

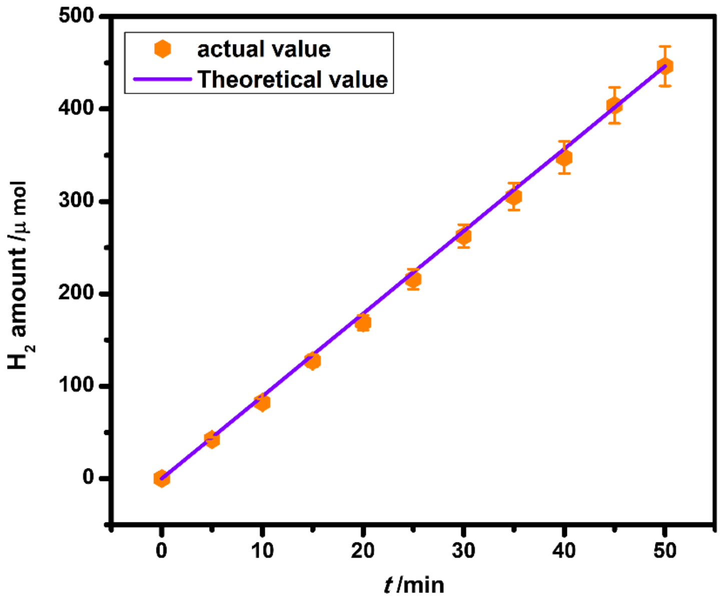

Figure S8. Electrocatalytic efficiency of $NiS_{0.25}$/CW for HER (at j =100 mA cm^{-2}) in 1.0 M KOH at 298 K.

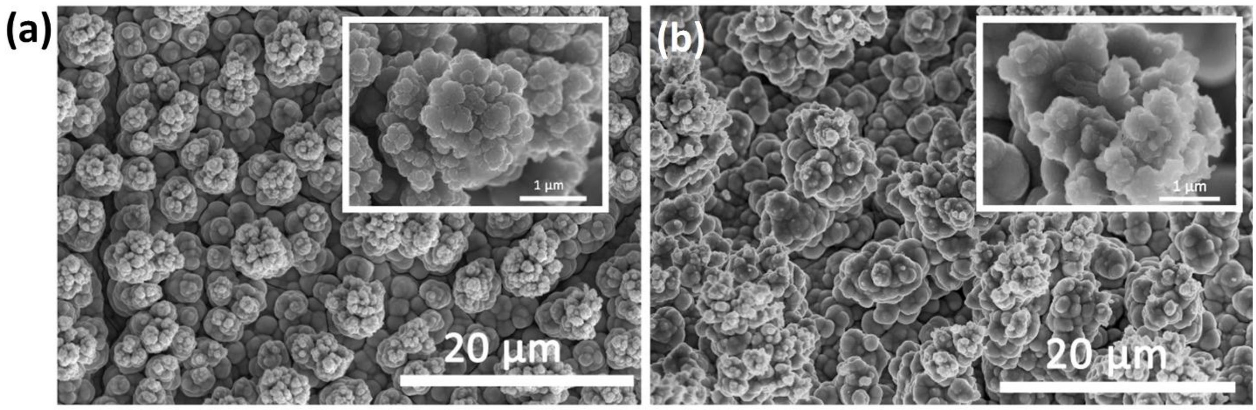

Figure S9. Comparison of SEM images of the $NiS_{0.25}$/CW (a) before and (b) after long-term HER (at j =10 mA cm^{-2} for 30 h) electrolysis in 1.0 M KOH at room temperature.

Table S3. Comparison of the HER performance of $NiS_{0.13}$/CW with other HER electrocatalysts in 1M KOH.

Catalyst	j (mA/cm^2)	$-\eta$ at the corresponding j (mV vs.RHE)	Tafel slope ($mV\ dec^{-1}$)	Refs
$NiS_{0.13}$/CW	10	54	54	**This work**
	50	104		
	100	135		
NiS_2 nanosheets/CC	2	78	104	1
	10	149		
Ni_3S_2 nanosheets/NF	10	123	110	2
	100	260		
Ni_3S_2 nanorods /AT-NF	10	200	107	3
Ni_3S_2 nanorods /NF	10	300	141	
Ni_3S_2 nanocomposites /CNT	10	340	167	4
Ni_3S_2 nanocomposite /MWCNT-NC	1.2	400	102	
	10	480		
	13	500		
Ni_3S_2 nanowires /NF	1	96	106	5
	10	199		
MoS_2/Ni_3S_2 /NF	10	199	88	6
NiS/NF	20	158	83	7
h-NiSx hierarchically porous/NF	10	60	99	8
NiS nanoframes/NF	10	94	139	9
Ni-S grade film	100	360	--	10
NiS Porous/ Copper plates	100	301	107	11
Ni/NiS/NF	10	230	123.3	12
Ni_3S_2@NPC/Cu film	10	60.8	67.5	13
	20	89.8		

References

1 C. Tang, Z. Pu, Q. Liu, A. M. Asiri and X. Sun, *Electrochim. Acta*, 2015, **153**,508-514.

2 C. Tang, Z. Pu, Q. Liu, A. M. Asiri, Y. Luo and X. Sun, *Int. J. Hydrogen Energy*, 2015, **40**, 4727-4732.

3 C. Ouyang, X. Wang, C. Wang, X. Zhang, J. Wu, Z. Ma, S. Dou and S. Wang, *Electrochim. Acta*, 2015, 297-301

4 T.-W. Lin, C.-J. Liu and C.-S. Dai, *Appl. Catal. B- Environ.*, 2014, **154-155**, 213-220.

5 J. Li, P. K. Shen and Z. Tian, *Int. J. Hydrogen Energy*, 2017, **42**, 7136-7142.

6 J. Zhang, T. Wang, D. Pohl, B. Rellinghaus, R. Dong, S. Liu, X. Zhuang and X. Feng, *Angew. Chem.*, 2016, **55**, 6702-6707.7.

7 W. Zhu, X. Yue, W. Zhang, S. Yu, Y. Zhang, J. Wang and J. Wang, *Chem. Commun.*, 2016, **52**, 1486-1489.

8 B. You and Y. Sun, *Adv. Energy Mater.*, 2016, **6**, 1502333.

9 X. Y. Yu, L. Yu, H. B. Wu and X. W. Lou, *Angew. Chem.*, 2015, **54**, 5331-5335.

10 K. Zhang, J. Liu, W. Xiao and C. Yan, *Mater. Lett*., 2017, 193, 77-80.

11 K. Zhang, W. Xiao, J. Li, J. Liu and C. Yan, *Electrochim. Acta*, 2017, **228**, 422-427.

12 G. F. Chen, T. Y. Ma, Z. Q. Liu, N. Li, Y. Z. Su, K. Davey and S. Z. Qiao, *Adv. Funct. Mater.*, 2016, **26**, 3314-3323.

13 C. Yang, M. Y. Gao, Q. B. Zhang, J. R. Zeng, X. T. Li and A. P. Abbott, *Nano Energy*, 2017, **36**, 85-94.